PROCEEDINGS OF SPIE

SPIEDigitalLibrary.org/conference-proceedings-of-spie

Wide-band self-collimation in low refractive index hexagonal lattice

Xia, Chun, Kuebler, Stephen, Martinez, Noel, Martinez, Manuel, Rumpf, Raymond, et al.

Chun Xia, Stephen M. Kuebler, Noel P. Martinez, Manuel Martinez, Raymond C. Rumpf, Jimmy Touma, "Wide-band self-collimation in low refractive index hexagonal lattice," Proc. SPIE 12010, Photonic and Phononic Properties of Engineered Nanostructures XII, 1201004 (5 March 2022); doi: 10.1117/12.2608627



Event: SPIE OPTO, 2022, San Francisco, California, United States

Wide-Band Self-Collimation in Low Refractive Index Hexagonal Lattice

Chun Xia^a, Stephen M. Kuebler^{a,b,c*}, Noel P. Martinez^a, Manuel Martinez^d, Raymond C. Rumpf^{d,e}, Jimmy Touma^f

^aCREOL, The College of Optics and Photonics, University of Central Florida, Orlando, FL 32816, USA

^bChemistry Department, University of Central Florida, Orlando, FL 32816, USA

^cDepartment of Materials Science and Engineering, University of Central Florida, Orlando, FL 32816, USA

dEM Lab, Department of Electrical and Computer Engineering, University of Texas at El Paso, El Paso, TX 79968, USA

^eComputational Science Program, University of Texas at El Paso, El Paso, TX 79968, USA ^fIntegrated Sensing and Processing Branch, AFRL/Munitions Eglin AFB, FL 32542, USA

ABSTRACT

We report a computational study of how light propagates within a self-collimating, hexagonal photonic crystal. The photonic crystal can be described as a two-dimensional hexagonal lattice of air holes extruded into the third dimension. While traveling inside the device, light is forced by self-collimation to propagate along the extrusion direction. Finite-difference time-domain calculations show that the lattice must have at least four rings of unit cells surrounding the innermost unit cells where light is centered for it to propagate under strong self-collimation, with low scattering loss.

Keywords: Self-collimation, photonic crystal, broad-band, multiphoton lithography, integrated photonics

1. INTRODUCTION

Photonic crystals (PCs) have a variety of applications in integrated photonics because of their bandgap (no allowed mode) [1] or dispersion properties within the band (allowed modes) [2, 3]. In-band dispersion revealed by the shapes of the bands provides abundant opportunities to control the flow of light. The dispersion properties can be visualized using isofrequency contours (IFCs). The shapes of the IFCs explain effects such as super-prism [3], negative refraction [4], slow light [5], and self-collimation (SC) [6]. SC arises at frequencies for which the IFCs are flat where light flows through a lattice with minimal beam spreading and is forced to follow a principal axis of the lattice. Moreover, by globally adding artificial spatial variation to lattices, power and phase can be independently controlled [7]. This effect can be engineered into a lattice using the spatially-variant-lattice algorithm (SVL) [8].

With multi-photon lithography (MPL), it is possible to fabricate SVLs of virtually any form. Two-dimensional (2D) self-collimators have been extensively explored [9-12]. However, three-dimensional (3D) self-collimators are limited [13], and the ones suitable for MPL are still lacking. If a lattice is to be fabricated by MPL, then additional constraints apply to the unit cell. The elements of the unit cell must be connected internally so the lattice survives lithographic development, and

*kuebler@ucf.edu Tele: +1 407-823-3720 Fax: +1 407-823-2252 http://npm.creol.ucf.edu

Photonic and Phononic Properties of Engineered Nanostructures XII, edited by Ali Adibi, Shawn-Yu Lin, Axel Scherer, Proc. of SPIE Vol. 12010, 1201004 © 2022 SPIE · 0277-786X · doi: 10.1117/12.2608627

the fill factor must be large enough to ensure structural integrity. Additionally, the performance of SC needs to be optimized if the lattice is to be fabricated from materials commonly used for MPL, like low refractive index photopolymers ($n \sim 1.5$).

Recently, a new type of 3D hexagonal lattice that exhibits strong SC was reported [6]. The unit cell of the lattice is shown in Fig. 1a. The lattice is unconventional because there is no periodicity along the direction light propagates. It was determined experimentally that this type of hexagonal lattice provides both broad bandwidth and strong SC with an input acceptance angle of up to 50°. Further, due to the lack of periodicity, SC occurs across multiple bands, enabling multimode operation. Unfortunately, deep understanding of how light propagates in such lattices is still lacking.

In this work, we report how light propagates in the hexagonal lattice of Fig. 1a based on findings obtained from finite-difference time-domain (FDTD) simulations performed using the MEEP tool-set [14]. The investigation reveals the minimum number of unit cell cells necessary for strong SC, and it provides insight into how power moves around within the lattice as light travels through the device.

2. SIMULATION SET UP

The diagram in Fig. 1(b) illustrates the setup for the FDTD simulation. The properties of the unit cell and the light source are the same as those reported in [6]. The solid purple line represents the size of the PC that was simulated. The lattice periodicity is $a=4.65~\mu m$. The hexagon-shaped unit cell is comprised of an air hole having radius r=0.35a in a uniform background having refractive index n=1.525. The lattice is periodic across the yz-plane. That cross-section is extruded into the third dimension along the x-direction by length L_x , along which light propagates due to SC. The PC is comprised of N rings of unit cells surrounding the hexagon in the center. The case where there is only one air hole in the center is denoted with N=0. The PC is illuminated by a Gaussian beam having a full-width-at-half-maximum (FWHM) of 9.5 μ m. The beam is centered on the input face of the lattice, with the electric field linearly polarized in the z-direction and a vacuum wavelength of $\lambda_0=1550$ nm. The source resides in an yz-plane positioned 1 μ m before the front surface of the PC and 1 μ m after the boundary layers. The boundaries are perfectly matched layers (PMLs) having a thickness of 1 μ m. Convergence was tested and verified by observing that the results did not change significantly when: (1) the thickness of the PML layer d_{PML} was increased from 1 μ m to 2 μ m, (2) the resolution was doubled from 10 elements per μ m to 20 elements per μ m, and (3) the total number of time steps was increased. Subsequent simulations were performed with the resolution set to 15 elements per μ m.

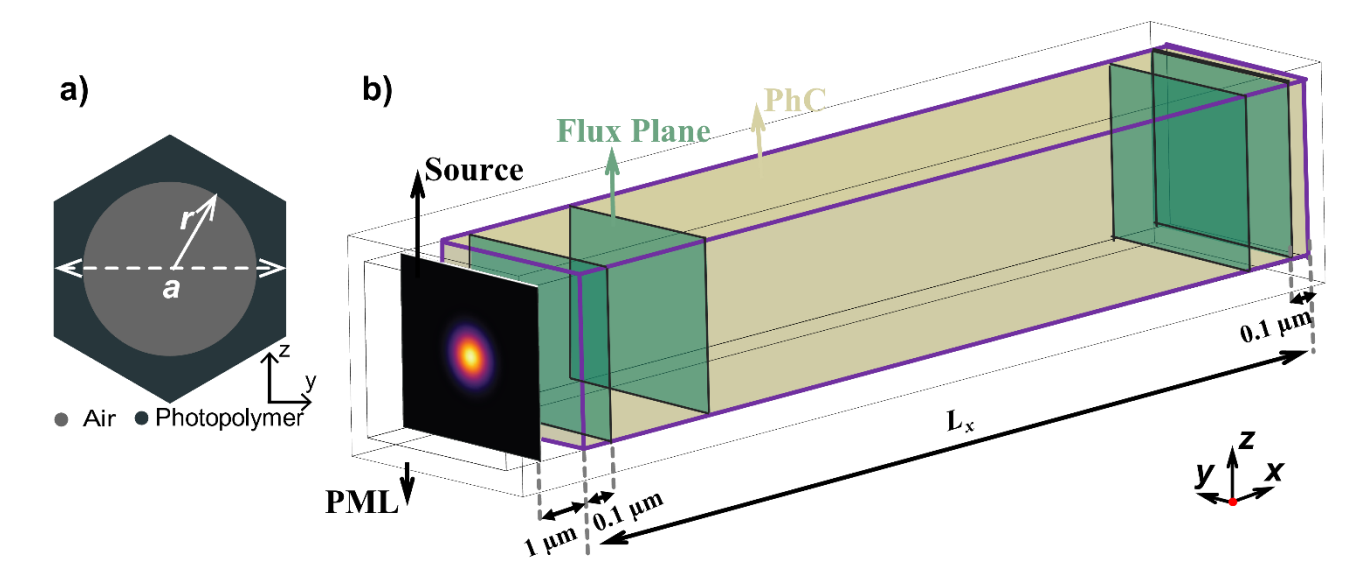


Fig. 1. (a) Unit cell comprising the hexagonal photonic crystal. (b) A schematic diagram showing the simulation setup for the FDTD simulations. The PC is inside the purple box and illuminated by a Gaussian beam positioned 1 μ m away from the front surface of the PC. The PML layers are along all directions with a thickness of 1 μ m. The green sheets are examples of planes along the *x*-axis at which energy flux is measured.

3. RESULTS AND ANALYSIS

The number of air holes needed to confine the light was studied. Five PCs having N increasing from zero to four but having the same $L_x = 30 \mu m$ were constructed. The PCs were simulated under the same conditions. Their intensity distributions are visualized at a common transverse yz-plane positioned 0.1 μm before the exit face of the PCs, and the results are plotted in Fig. 2.

The minimum layers of unit cells needed to enable SC is related to the width of the light source. In this case, the input beam has a FWHM of 9.5 μ m. The total power captured by the 0th, 1st, and 2nd rings of unit cells is 25%, 60%, and 12%, respectively. So, the center and the first two rings of unit cells capture 97% of the total input power. Based on this finding, it is reasonable to assess the strength of SC versus the number of rings surrounding the central ring and to ask what minimum number of rings is needed to prevent energy from leaking beyond the 2nd ring.

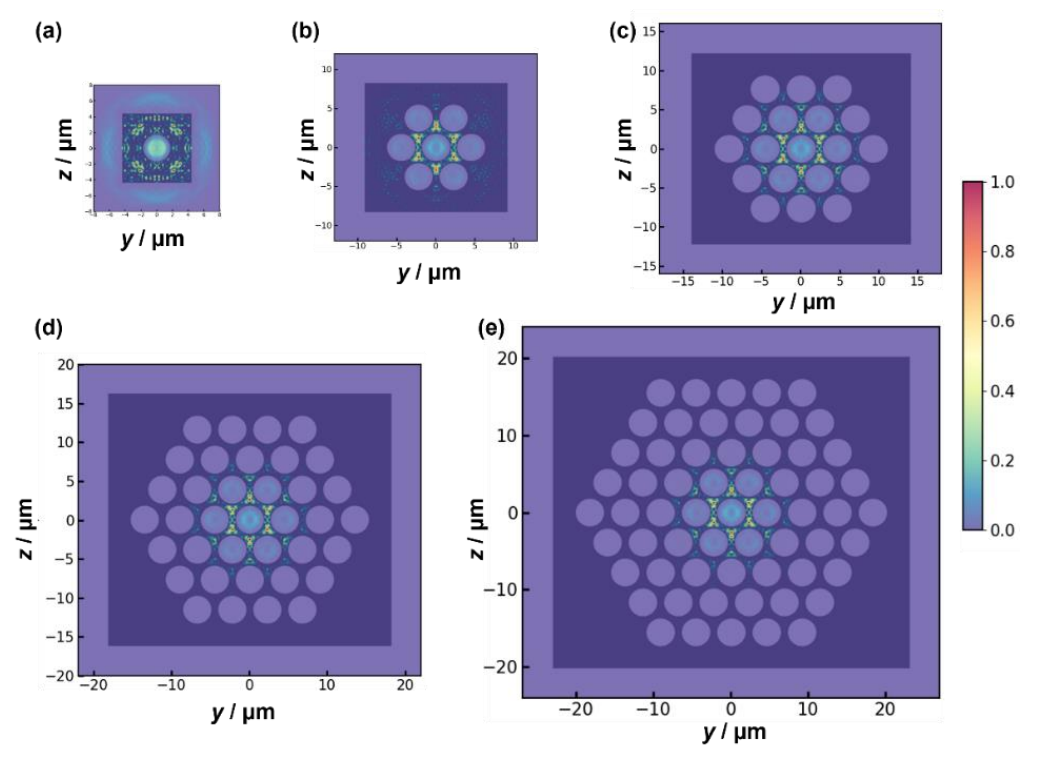


Fig. 2. The intensity profile along the yz-plane is visualized at 0.1 μ m before the ending of the PC along the x-direction for five PCs. Panels (a) - (e) correspond to N = 0, 1, 2, 3, and 4.

Figure 2(a) illustrates the profile of a PC with a single unit cell in the center (N=0). Due to the absence of any kind of PC, there is an apparent leakage of light from the center unit cell. Figures 2(b) - 2(e) illustrate that power leakage decreases as N increases. At $N \ge 3$, the leakage is minimal. The conclusion is therefore drawn that at least three rings of unit cells are required around the illumination center for effective SC. Furthermore, it is noteworthy that the beam profile shown in Fig. 2(b) is beginning to resemble that shown in Fig. 2(c) - 2(e), with as few as one ring of unit cells.

A PC composed of three rings of unit cells and having $L_x = 60 \,\mu\text{m}$ was used to study how power moves within the lattice as light propagates through the device. In Figure 3, panels b(1) - e(2) identify the areas where power flux was measured. Sets 3b, 3c, 3d, and 3e represent rings N = 0 to 3. Within each ring, power flux was integrated over the air- and material-regions separately, as identified in yellow. The integrated flux in these areas was measured versus x to provide insight into how power moves between different regions of the lattice as the light propagates. Inspection of Figure 3 shows that power continuously oscillates between air (solid dots) and material (solid stars) but remains strongly confined to primarily rings zero and one. Fourier analysis shows that the spatial oscillation frequency is $0.32 \text{ cycles/}\mu\text{m}$ and is constant up to N = 2.

Light that escapes from the second ring of unit cells oscillates at a slower spatial frequency and represents only 5% of the total power.

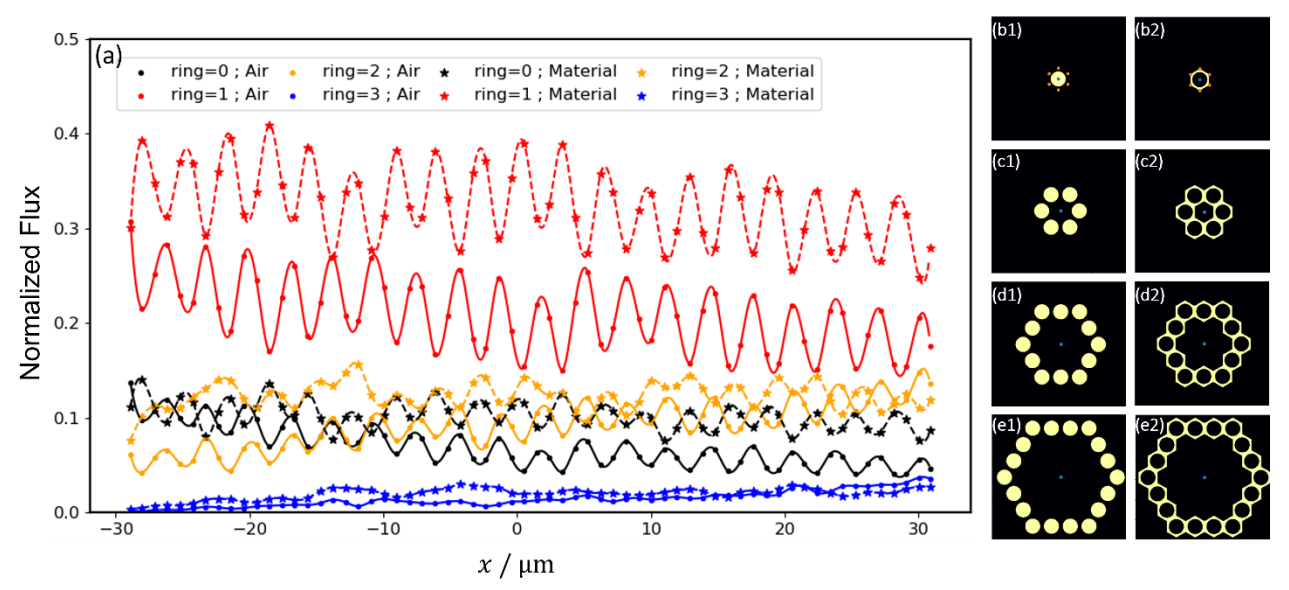


Fig. 3. (a) Normalized power exchanging between air and the material within the *N*th ring of the lattice. The power contained within air is denoted by solid dots. The power contained in the material is denoted by stars. The colors black, red, yellow, and blue identify energy in the 0th, 1st, 2nd, and 3rd rings, respectively. Panels (b) through (e) identify the air- and material-zones for which power flux is integrated for each of the *N* rings.

4. CONCLUSION

We investigated how light propagates in a new type of 3D hexagonal PC using FDTD simulations. We demonstrate that the lattice exhibits strong SC, and as little as two rings of hexagonal unit cells are needed to confine an incident Gaussian beam having a FWHM of $9.5~\mu m$. It is found that power oscillates between regions of air and material as light propagates along the extrusion axis. The strong SC-property of this lattice makes it a good candidate for new types of integrated photonic devices based on spatially-varied lattices.

5. ACKNOWLEDGMENTS

This work was partly supported by the Air Force Research Laboratory (FA8651-19-1-0003) and National Science Foundation grants no. 1711356 and 1711529. Distribution approved for public release, distribution unlimited (96TW-2021-4417).

References

- [1] S. Noda, A. Chutinan, and M. Imada, "Trapping and emission of photons by a single defect in a photonic bandgap structure," Nature, 407(6804), 608 (2000).
- [2] L. Wu, M. Mazilu, and T. F. Krauss, "Beam steering in planar-photonic crystals: from superprism to supercollimator," Journal of lightwave technology, 21(2), 561 (2003).
- [3] H. Kosaka, T. Kawashima, A. Tomita *et al.*, "Superprism phenomena in photonic crystals," Physical Review B, 58(16), R10096 (1998).
- [4] Q. Zhu, Y. Fu, Z. Zhang *et al.*, "Negative refraction and focusing of photonic crystals with graded negative index in visible regime," Plasmonics, 8(2), 335-340 (2013).
- [5] T. Baba, "Slow light in photonic crystals," Nature Photonics, 2(8), 465 (2008).
- [6] C. Xia, S. M. Kuebler, N. P. Martinez *et al.*, "Wide-band self-collimation in a low-refractive-index hexagonal lattice," Optics Letters, 46(9), 2228-2231 (2021).

- [7] J. J. Gutierrez, N. P. Martinez, and R. C. Rumpf, "Independent control of phase and power in spatially variant self-collimating photonic crystals," JOSA A, 36(9), 1534-1539 (2019).
- [8] R. C. Rumpf, and J. Pazos, "Synthesis of spatially variant lattices," Optics Express, 20(14), 15263-15274 (2012).
- [9] Y. Chuang, and T. Suleski, "Photonic crystals for broadband, omnidirectional self-collimation," Journal of Optics, 13(3), 035103 (2011).
- [10] Z. Wu, K. Xie, H. Yang *et al.*, "All-angle self-collimation in two-dimensional rhombic-lattice photonic crystals," Journal of Optics, 14(1), 015002 (2011).
- [11] R. E. Hamam, M. Ibanescu, S. G. Johnson *et al.*, "Broadband super-collimation in a hybrid photonic crystal structure," Optics Express, 17(10), 8109-8118 (2009).
- [12] P. T. Rakich, M. S. Dahlem, S. Tandon *et al.*, "Achieving centimetre-scale supercollimation in a large-area two-dimensional photonic crystal," Nature Materials, 5(2), 93 (2006).
- [13] R. Iliew, C. Etrich, and F. Lederer, "Self-collimation of light in three-dimensional photonic crystals," Optics Express, 13(18), 7076-7085 (2005).
- [14] A. F. Oskooi, D. Roundy, M. Ibanescu *et al.*, "MEEP: A flexible free-software package for electromagnetic simulations by the FDTD method," Computer Physics Communications, 181(3), 687-702 (2010).